Digest Journal of Nanomaterials and Biostructures Vol. 10, No. 2, April - June 2015, p. 429 - 436

GMR ON CuNiCo THIN LAYERS DEPOSITED USING TVA METHOD

I. PRIOTEASA[a], C. POROSNICU[b*], C.P. LUNGU[b], I. JEPU[b], G. SCHINTEIE[c], V. CIUPINA[a,d], G.PRODAN[d], E. VASILE[e], P. DINCA[b]
[a]*University of Bucharest, Romania*
[b]*National Institute for Laser, Plasma and Radiation Physics, Magurele, Romania*
[c]*National institute for Material Physics, Magurele, Romania*
[d]*Research Center on Micro-and Nanostructures, Ovidius University of Constanta, Romania*
[e]*METAV Bucharest*

Thermionic vacuum arc was successfully used to prepare high quality nanostructure thin films with different fields of applicability. One advantage of this deposition technique was the ability to have a controlled range of thicknesses starting from few nanometers to hundreds of nanometers. The purity of the thin films was insured by a high vacuum pressure and a lack of any kind of buffer gas inside the coating chamber. The aim of this work was to obtain significant magnetic response and to compare the MR to the structures obtained for two different granular combinatorial structures. The samples were investigated using scaning and transmision electron mycroscopy while SEM and The magnetic properties were first studied by measuring the electrical resistance behavior for a magnetic field of 0.3 T, at different values of the sample temperature and using a non-destructive optical method called Magneto-Optical Kerr Effect (MOKE). The magnetoresistive effect obtained for the studied samples varied from 0.6% to 19% in respect sample structure and temperature for a constant magnetic field.

(Received February 14, 2015; Accepted April 24, 2015)

Keywords: Thermionic vacuum arc; Giant Magnetoresistive (GMR); Magneto-Optical Kerr Effect (MOKE)

1. Introduction

High interest is shown lately for magnetoresistive structures and used in the magnetic memory technology. An improvement to the memory devices is crucial due to the market demand to increase the reading speed and storage capacity for kind of devices. Studies on this type of thin films were developed by research teams from all over the world especially for their electric and magnetic properties. The magnetoresistance effect consists of decreasing the electric resistance of a conductor material when subjected to a magnetic field. I. Mustata and others [1,10] reported a magnetoresistance effect of up to 33% for the films obtained by TVA method, and F. Wang [11] obtained a magnetoresistance effect of 6,2% in the case of CuNiCo thin structure at room temperature. A decrease of the magnetoresistance effect was observed for the samples which were thermally treated at 600^0C.

In the present work, a 30000 spires electromagnet was used to generate a magnetic field with values between 0.3 T and 0.36 T. The sample was introduced in a vacuum cryostat between the poles of the electromagnet. Its electric resistance was measured both in the absence and the presence of the magnetic field, and which was applied perpendicular on the sample. A significant decrease of the electrical resistance was noticed after applying the magnetic field. A total thickness of the thin film was 36 nm which was obtained by thermal evaporation in a high vacuum enclosure at - $8x10^{-6}$ Torr pressure. The structure was a multilayer type composed of 4 magnetic matrices (in

* Coresponding author: corneliu.porosnicu@inflpr.ro

our case two of Co and two of Ni) with an individual thickness of 5 nm, separated by 4 non magnetic ones (Cu), with an individual thickness of 4 nm. The diameter of the magnetic nanograins (Ni and Co) present in the Cu matrix of the structure was determined using a transmission electron microscope [12].

2. Experimental set-up

In order to obtain the desired structure, two anode-cathode TVA systems were used [13,14]. As it can be seen from the fig.1 one anode-cathode system was used for the evaporation of cooper. For the magnetic materials, it was used a special anode with a circular rotary graphite disk. On this were placed two graphite crucibles, each containing Ni and Co respectively. With a mechanical arm, each crucible was placed into the right position under the cathode.

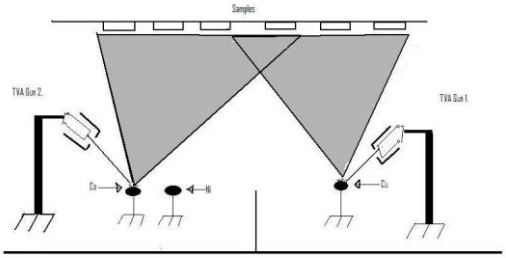

Fig.1. The schematic view of the TVA with two anode-cathode systems

Fig.2 Schematic view of the multilayer structure

Six samples were placed along the two anode-cathode systems, at a distance of about 25 cm above each of them. The multilayer structure consisted in 8 individual layers, as presented in the fig.2. The non magnetic layers represented by cooper had a thickness of 4 nm, and the magnetic layers represented by Ni and Co respectively had an individual thickness of 5 nm each. The total thickness of the obtained structure was of 36 nm.

The working parameters of the thermionic vacuum arc discharges for this experiment were: In the case of the Cu, the cathode which consisted of a tungsten filament placed into a Wehnelt cylinder was heated up by a current with a value of $I_{filament}$=50A, The discharge current had a value of I_{desc}=150mA, and the applied voltage on the anode was of U=1300V. Keeping constant these discharge parameters, it was obtained a deposition rate=0,2-0,4Å/s which was measured in-situ using a micro-quartz balance. For nickel plasma, the parameters were: $I_{filament}$=55A, I_{disch}=400mA, U_{disch}=1000V, deposition rate=0,2-0,3Å/s.
In the case of Co, $I_{filament}$=1600V, I_{disch}=400mA, U_{disch}=55A, deposition rate=1,2Å/s. The working pressure was of $8x10^{-6}$Torr.

To carry out the magnetoresistance measurements, the samples were introduced in a vacuum cryostat which in its turn was introduced between the poles of an electromagnet. A current of 5 mA was applied on the samples. In addition, a standard resistance of 10 ohms was introduced in the circuit.

3. Results and discussions

The morphology of the samples is very important from the MR point of view due to the fact that magnetic structures are very sensitive to the layer stucture in terms or thicknesses of each layer of the TMR structure, as well as their purity and to the concentration of the grains embedded in a non-magnetic matrix for a GMR structures [9,15,16]. This why, they were initialy studied using a Philips CM120ST transmission electron microscope. Fig 3 shows the CuNiCo structure of

the sample P_1 placed above the Ni-Co anode-cathode system magnified 18000 times, and figures 4a and 4b present the distribution of the ferromagnetic grain diameters for samples P_1 and P_2 respectively. It can be observed that the majority of the grains have dimensions in the range of 12 to 14 nanometers for sample P1 while for sample P_2 the grainsize increased to 40-55 nm. The experimental curve was fitted with a function given by y0+a*exp(-ln(x/xc)*ln(x/xc)/(2*w*w)) where y_0 is the base line, it represents a constant which depends on the number of particles, xc is the value of the maximum and w the dispersion. The function was chosen assuming that the distribution of the nanograins is lognormal.

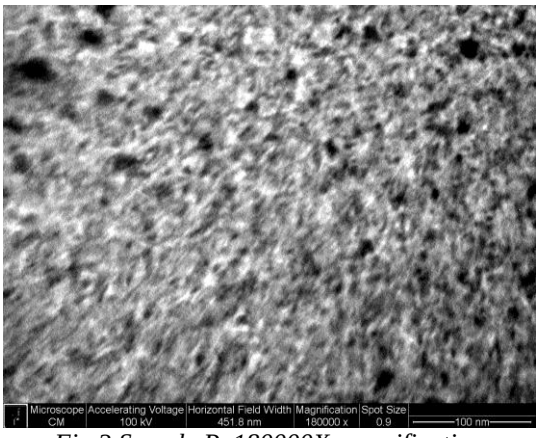

Fig.3 Sample P_1 180000X magnification

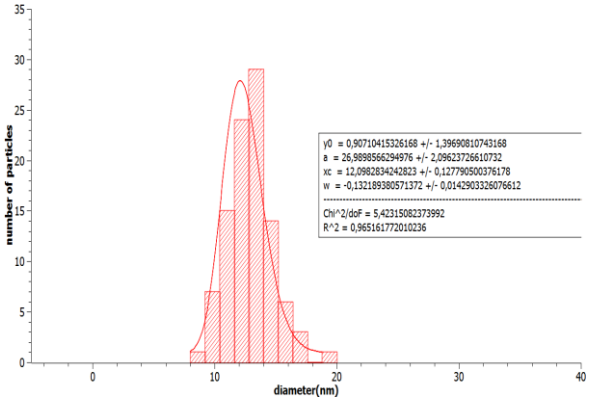

Fig.4a The distributions of grain diameters for P_1

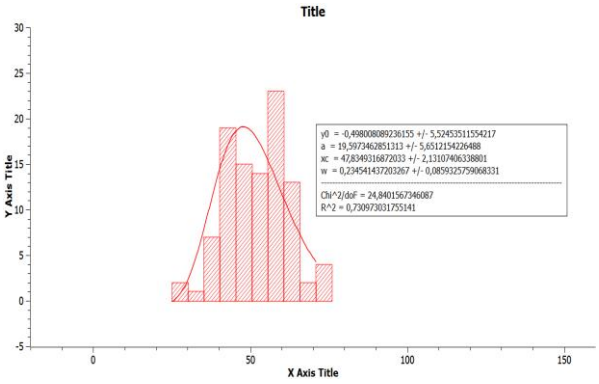

Fig. 4b. The distribution of grain diameters for P_2

Fig. 5 shows SEI images (secondary electrons images) obtained both on the surface of the sample and on its section with the help of the Quanta Inspect F environmental scanning electron microscope. Quanta Inspect F has a filament with field emission and a linear resolution of 1,4 nm. The resolution of the device was affected by the nature of the sample (glass) which charges electrostatically and does not allow seeing the successive layers of CuCoNi separately. In order to obtain the SEI image in section the sample was fractured.

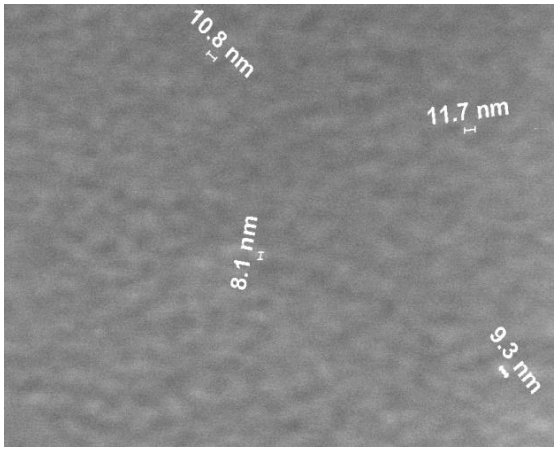

Fig.5.a). SEI image on surface

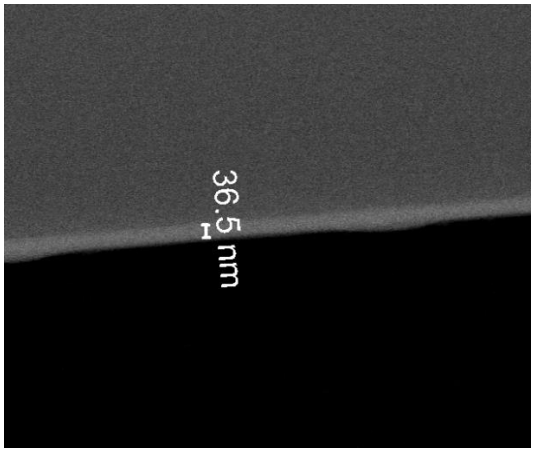

Fig.5.b). SEI image in section

EDAX analysis shows the characteristic X rays emitted by the sample on the impact of the electron beam with the analyzed structure. The measurements offer spectra of characteristic X rays with dispersion in energy. The OX axis in the plot represents the energy of the detected X radiations. OY axis shows the intensity (the number of impulses).

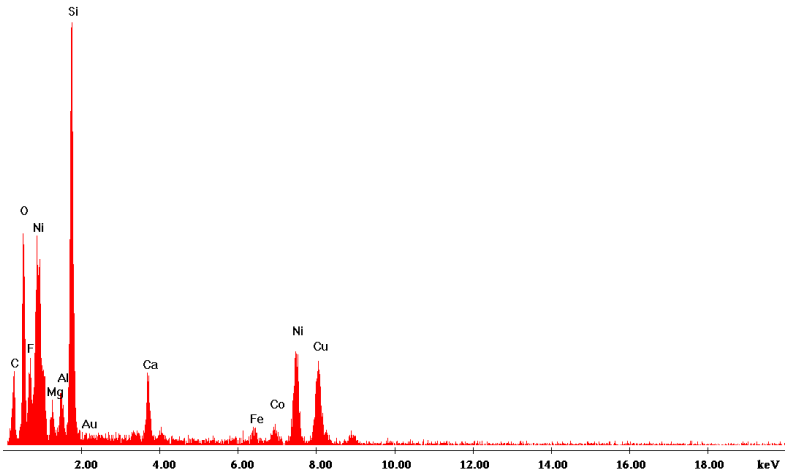

Fig.6 The EDAX image of the CuNiCo film

Fig. 6 shows an EDAX image obtained on the CuNiCo film where we can notice the existence of the 3 deposited elements: Cu, Ni, Co and as minority element Fe (probably impurities from the processing). The other detected elements are present due to the glass and silicon substrate on which the films were deposited.

Magnetoresistance effect measurements were performed on the CuNiCo structure. The samples were placed in a high vacuum cryostat, which in its turn was introduced between the poles of an electromagnet.

The cryostat pressure was of approximately $3x10^{-4}$ Torr. The R_x resistance was firstly measured, in the absence of the magnetic field B=0, and then in the presence of a magnetic field. The measurements were carried out firstly at room temperature and then the temperature on the sample was progressively increased until the value of 75 Celsius degrees was reached. In the presence of the magnetic field it was noticed a decrease of the electric resistance of the sample

To determine R_x the following relation was used: $R_x = R_e \frac{U_{R_x}}{U_{R_e}}$, where U_{Rx} represents the dropping voltage value measured on the sample and U_{Re} represents the dropping voltage value measured on the standard resistance. The standard resistance has to be corrected in order to avoid temperature related measuring errors, using the formulae: $R_e=10\Omega(1+\frac{1}{273}xT^0C)$ where T is the temperature of the sample which has been modified during the measurements starting with 30^0C up to 75^0C. In fig 7 the schematic representation of the measuring circuit presented.

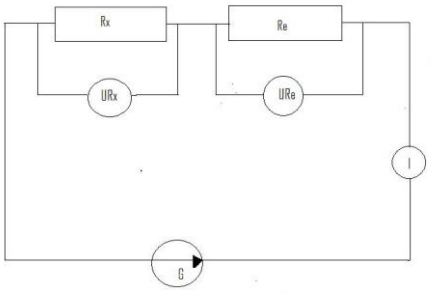

Fig. 7. The schematic representation of the measuring circuit

Magnetoresistance was calculated by using the relation: $MR(\%)=\frac{\Delta R_x}{R_0}$ x100%, where $\Delta R=R_x-R_o$, with Rx = the sample resistance in the presence of the magnetic field and R_0 the value of the resistance in the absence of the magnetic field.
In fig 8 it can be observed the magnetoresistive effect obtained on sample P_1, For this particular sample, the ferromagnetic grain diameter was found to be 14 nm. At 335^0K a value of -0,6370% was obtained, after that the temperature was repeatedly increased up to the temperature of 365^0K, where it can be observed a significant variation of it together with magnetic field modification, the maximum being -19,13% at an applied magnetic field of 0,3549T.

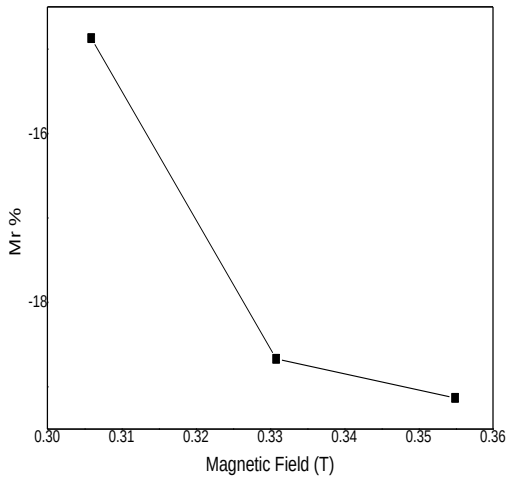

Fig.8 The magnetoresistive effect measured on sample P_1

Another sample which presented a special magnetoresistive effect was sample P_2 with the dimensions of the grains around 50 nm. In the below figure we have the distribution of the diameters corresponding to sample P_2.

The sample P_2, for which the ferromagnetic grain size embedded in the cooper matrix, was found to be 40-50 nm showed a magnetoresistance effect both positive and negative depending samples temperature as it can be seen in fig. 9. For this probe, the MR effect had a lower value than in the case of sample P_1. It can be deduced that a greater value of the ferromagnetic grains diameters affects the MR effect. The electronic spins of the magnetic domains within the sample P_2 have a more defined orientation, being harder to be reoriented, thank in the case of sample P_1, which presents lower values of the ferromagnetic grains diameters.

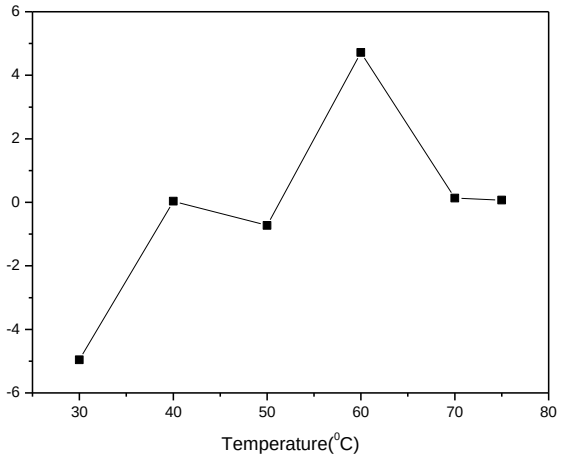

Fig.9 The temperature dependence of the magnetoresistive effect measured on sample P_2

MOKE measurements were performed on both samples P_1 and P_2. The magnet - optical Kerr effect (Moke) describes the interaction between the electromagnetic waves and magnetic materials, fact that corresponds to the rotation or to the change of the intensity of the light linear polarized through the reflection of the magnetic materials placed in a magnetic field. The Kerr effect is proportional to the magnetization of the magnetic materials.
In figure 10 it can be seen the Moke signal for sample P_1. with both responses from Co and Ni. The Kerr rotation angle was 0,8714 mdeg, the residual magnetization 1,4649 mdeg, and the coercive field is of 10 Oe coresponding to Ni and 30 Oe which corresponds to Cobalt

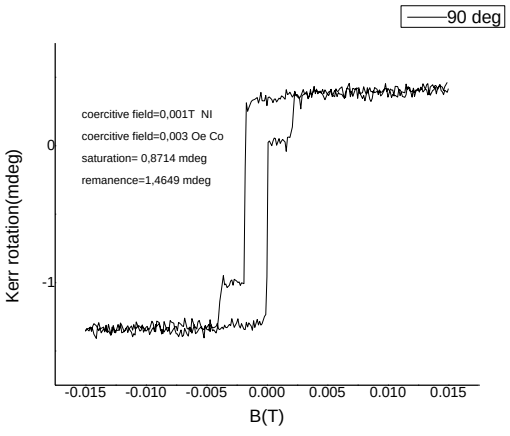

Fig.10 The Moke signal corresponding to sample P_1

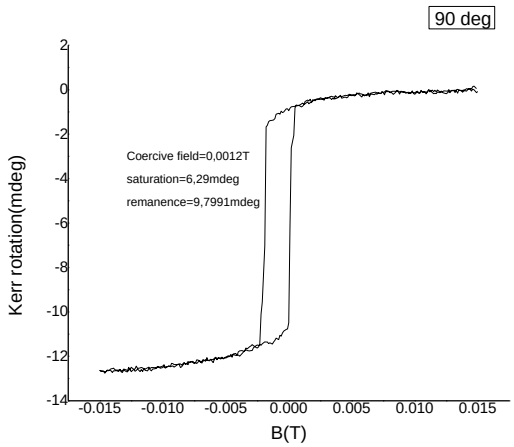

Fig.11. The Moke signal corresponding to sample P_2

Figure 11 illustrates the MOKE signal corresponding to sample P_2. As it can be observed the two ferromagnetic components are not clearly emphasized in the cycle. The coercive field was

approximately 12 Oe and the recorded MOKE signal of about -10 mdeg. It is shown that MOKE measurements were in perfect concordance with the magnetoresistance measurements .

4. Conclusions

Thermionic vacuum arc was successfully used to obtain high quality ferromagnetic structures. TEM measurements on two of the samples showed a variation of the grain size diameters of the magnetic materials used (Ni and Co) embedded in the non magnetic cooper matrix. This variation had a strong influence of the samples. A relative maximum of 19.13% in the change of the electric resistance was observed for sample P_1, at a constant temperature of 365K. MOKE measurements were a confirmation of the GMR effect- obtained on this multilayer ferromagnetic structure.

A higher Ni Co concentration from the Cu matrix allowed reaching some quite high values of magnetoresitance, therefore we can talk about a GMR effect. Through direct measurements it has been noticed that the magnetoresistive effect obtained on sample P_1 was bigger than that on sample P_2. A decisive factor was the diameter of the grains, which in sample P_1 was of only 12-14 nm in comparison with sample P_3 which had diameters up to 50 nm, this significantly affecting the magnetoresistive effect of the sample.

Acknowledgements

This work was supported by a grant of the Romanian National Authority for Scientific Research, CNDI– UEFISCDI; project number 160/2012, PN-II-PT-PCCA-2011-3.2-1453

References

[1] Mustata, C.P. Lungu, A.M. Lungu, V. Zaroski, M. Blideran, V. Ciupina, Vacuum, **76**(2–3), 131 (2004).
[2] V. Kuncser, G. Schinteie, P. Palade, I.Jepu I. Mustata, C.P. Lungu, F. Miculescu, G. Filoti Journal of Alloys and Compounds, **499**(1),23 (2010).
[3] V. Kuncser, M. Valeanu, G. Schinteie, G. Filoti, I. Mustata, C.P. Lungu, A. Anghel, H. Chiriac, R. Vladoiu, J. Bartolome, Journal of Magnetism and Magnetic Materials, **320(**14), 226 (2008).
[4] V. Stancu, C. Dragoi, V. Kuncser, G. Schinteie, L. Trupina, E. Vasile, L. Pintilie, Thin Solid Films, **519**(19), 6269 (2011).
[5] C. Kuncser, A. Kuncser, G. Maftei, S. Antohe, Procedia, Social and Behavioral Sciences, **46**, 5324 (2012).
[6] V Kuncser, M Rosenberg, G Principi, U Russo, A Hernando, E Navarro, G Filoti, Journal of Alloys and Compounds, **308**(1–2), 21 (2000).
[7] V. Raghavendra Reddy, O. Crisan, Ajay Gupta, A. Banerjee, V. Kuncser, Thin Solid Films, **520**(6), 2184 (2012).
[8] I. Mihalca, A. Ercuta, I. Zaharie, A. Jianu, V. Kuncser, G. Filoti, Journal of Magnetism and Magnetic Materials, **157–158,** 161-162(1996)
[9] V. Kuncser, I. Mustata, C.P. Lungu, A.M. Lungu, V. Zaroschi, W. Keune, B. Sahoo, F. Stromberg, M. Walterfang, L. Ion, G. Filoti, Surface and Coatings Technology, **200**(1–4), 980 (2005).
[10] C. T. Fleaca, F. Dumitrache, I. Morjan, R. Alexandrescu, C. Luculescu, A. Niculescu, E. Vasile, V. Kuncser, Applied Surface Science, **278**, 284 (2013).
[11] F. Wang, T. Zhao, Z. D. Zhang, M. G. Wang, D. K. Xiong, X. M. Jin, D. Y. Geng, X. G. Zhao, W. Liu, M. H. Yu, F. R. de Boer, J. Phys. Condens. Matter, **12**(11), 2525 (2000).
[12] R. M. Oksuzoglu, T. E. Weirich, H. Fuess, Journal of Electron Microscopy, **52**(2), 91 (2003)

[13] A. Marcu et al., Thin Solid Films **519,** 4074 (2011).
[14] I. Jepu, C. Porosnicu, I. Mustata, C.P. Lungu, V. Kuncser, F. Miculescu, Romanian Reports in Physics **62**, 771 (2010)
[15] I. Jepu, C. Porosnicu, I. Mustata, C.P. Lungu, V. Kuncser, M. Osiac, G. Iacobescu, V. Ionescu, T. Tudor; Rom. Rep. Phys., **63,** 804 (2011).
[16] A. Anghel, C.P. Lungu, I. Mustata, V. Zaroschi, A.M. Lungu, I. Barbu, M. Badulescu, O. Pompilian, G. Schinteie, D. Predoi, V. Kuncser, G. Filoti, N. Apetroaei; Czech. J. Phys., **56,** 16 (2006).